

Synthesis of Spirocyclic Diphosphite-Supported Gold Metallomacrocycles via a Protodeauration/Cyclization Strategy: Mechanistic and Binding Studies

Lindsay J. Schafer,[†] Kevin J. Garcia,[†] Andrew W. Baggett,[‡] Taylor M. Lord,[†] Peter M. Findeis,[†] Robert D. Pike,[§] and Robert A. Stockland, Jr.*[†]

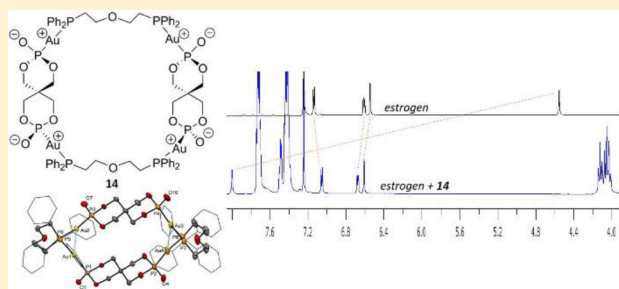
[†]Department of Chemistry, Bucknell University, Lewisburg, Pennsylvania 17837, United States

[‡]Department of Chemistry, Linfield College, McMinnville, Oregon 97128, United States

[§]Department of Chemistry, The College of William and Mary, Williamsburg, Virginia 23187, United States

S Supporting Information

ABSTRACT: A spirocyclic diphosphite was used to generate P-metalated bimetallic complexes through protodeauration reactions involving $\text{LAuC}_6\text{H}_4\text{tBu}$ ($\text{L} = \text{JohnPhos}$, tBuXPhos) and metallomacrocycles through protodeauration/cyclization using $\text{tBuC}_6\text{H}_4\text{AuP}^{\wedge}\text{PAuC}_6\text{H}_4\text{tBu}$ precursors ($\text{P}^{\wedge}\text{P} = \text{flexible diphosphine}$). While the synthesis of the bimetallic complexes followed a stepwise process, generation of the metallomacrocycles was highly complex because of a series of reversible ligand redistribution reactions. The self-assembly was monitored, and key intermediates were identified by NMR spectroscopy and high-resolution mass spectrometry. The mechanistic investigation showed that using flexible diphosphine linkers was critical to the selective synthesis of metallomacrocycles because rigid diphosphines generated intractable mixtures of linear and cyclic compounds. The X-ray structure of a 32-membered metallomacrocyclic revealed that the compound crystallized in an unsymmetrical collapsed form that was held together by two supported aurophilic interactions while the flexible diphosphines were folded along opposite sides of the metallomacrocyclic. The solution structure was consistent with a symmetric species, which suggested interconversion between an open and collapsed form and/or rapid twisting of a collapsed form. The 32-membered metallomacrocyclic was used to bind estrogen primarily through the formation of $\text{AuP}-\text{O}^-\cdots\text{H}-\text{OR}$ hydrogen bonds.



INTRODUCTION

The selection of the linker remains a critical choice in the design of a new metallomacrocyclic or metal–organic framework (MOF). While a host of functional groups have been used to link metal centers, phosphonates remain a popular choice.^{1–4} The majority of phosphonate-based linkers found in metallomacrocyclics and MOFs use the oxygen atoms from the RPO_3^{2-} groups to bind metal centers.⁵ With the noteworthy exception of pyrophosphite and its derivatives,^{6,7} using phosphonates and related compounds to link metal centers through $\text{M}-\text{P}$ bonds has received less attention and could generate frameworks and architectures with unique geometries and unconventional substrate binding sites. The well-known Kläui ligand is the small-molecule version of this approach.^{8–10} This cobalt-based metalloligand provides an all-oxygen donor environment and has been used to bind a variety of metals including lanthanides and actinides,^{11–13} transition metals,^{14,15} and main-group elements such as bismuth.¹⁶ Furthermore, there is considerable interest in the preparation of dynamic coordination polymers, metallomacrocyclics, and MOFs.^{17,18} One approach to the construction of these systems entails the use of both rigid and flexible components.^{17–20} Extending this

chemistry to well-defined coordination architectures based upon phosphorus-metalated $\text{M}[\text{PO}_3\text{R}_2]$ fragments has been challenging, partly because of the paucity of precursors.

To this end, we surmised that the spirocyclic diphosphite (**1**, shown in Figure 1 in its hydrogen phosphonate form) and its derivatives could be effective “rigid” linkers for metallomacrocyclics and MOFs.²¹ Indeed, tertiary phosphites based upon a pentaerythritol core have been used to generate dinuclear complexes and coordination polymers.²² One of the common methods used for the preparation of late-metal-containing

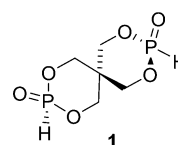


Figure 1. Spirocyclic linker for the construction of phosphorus-metalated coordination architectures.

Received: June 29, 2018

metallomacrocycles and MOFs utilizes a metal precursor bearing a weakly coordinating ligand such as water, nitrate, or solvent.^{23–26} Displacement of this poorly held ligand from the metal by a donor from the linker is a key step in the self-assembly process, and a staggering array of metallomacrocycles and MOFs have been generated using this methodology. Linker **1** could be used for such a process if the hydrogen phosphonate form shown in Figure 1 tautomerized to a secondary phosphite. Although the equilibrium favors the hydrogen phosphonate form in solution,^{27,28} the phosphite form can be trapped by a metal center.⁶ If the newly attached metal center contains a sufficiently basic group that was able to remove the hydrogen from the MPOH fragment (protodemetalation),^{29–33} it would generate a formally neutral connection between the metal and linker. One version of this approach begins with an organometallic fragment and eliminates a small organic molecule that can be easily removed by evaporation or extraction. Schmidbaur and our group reported that organogold compounds are quite susceptible to protodeauration using reagents bearing labile P–H groups.^{34–37} Building on this, we have investigated the susceptibility of **1** to generate well-defined frameworks/architectures upon treatment with suitable dinuclear organogold precursors.

RESULTS AND DISCUSSION

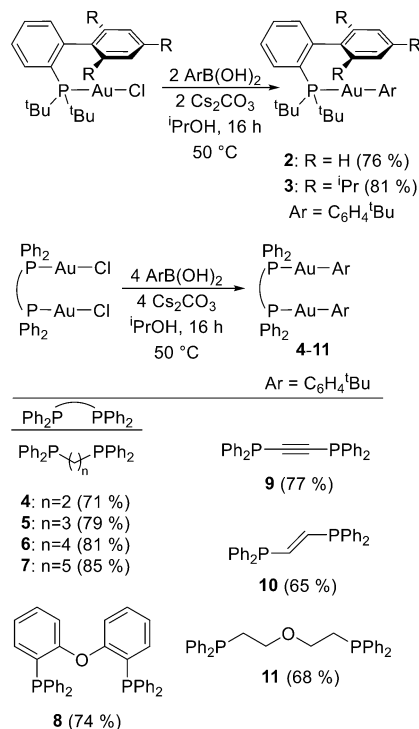
Synthesis of Arylgold Precursors. The approach to the preparation of the arylgold precursors is summarized in Scheme 1. For both the mononuclear and dinuclear gold substrates, the treatment of R_3PAuCl or $(Ph_2P^APh_2)Au_2Cl_2$ with 4-*tert*-butylphenylboronic acid along with cesium carbonate generated arylgold precursors (**2–11**) in moderate yields.^{38–40} The 4-*tert*-butylphenyl ($C_6H_5^tBu$) group was selected for this chemistry because it was easy to observe/

follow using 1H NMR spectroscopy when monitoring the protodeauration reactions (vide infra). The bulky dialkylbiarylphosphines were used because of their ability to inhibit the dynamic solution behavior³⁴ and to provide a model system for the reaction of **1** with arylgold species. The diphosphines shown in Scheme 1 were chosen in order to provide flexibility or rigidity to the coordination architectures. All of the arylgold precursors exhibited a singlet in the $^{31}P\{^1H\}$ NMR spectrum and were isolated as off-white solids.

The molecular structures of **9** and **10** were determined by X-ray crystallography (Figure 2). In general, diphosphine-linked dinuclear gold compounds tend to crystallize in one of three forms: macrocycle, folded polymer, and a stretched (open) polymer, where the gold compounds are held together by noncovalent interactions such as hydrogen-bonding and aurophilic interactions.^{41,42} It is often unpredictable which form will crystallize and whether or not close $Au\cdots Au$ contacts will be observed. Crystals of **9** were grown by cooling a saturated dichloromethane (CH_2Cl_2)/tetrahydrofuran (THF) solution to $-10\text{ }^\circ C$. After several days, colorless crystals were isolated by filtration. Compound **9** crystallized in the triclinic system $P\bar{1}$ with two independent molecules of **9** per asymmetric unit. The P–Au–C angles are between $167.49(8)$ and $174.77(8)^\circ$, the Au–C bond lengths are between $2.043(3)$ and $2.048(3)$ Å, and the Au–P distances are between $2.2814(7)$ and $2.3000(7)$ Å. Compound **9** aggregated into 12-membered metallomacrocycles using two molecules of **9**. Noncovalent (aurophilic) interactions were found between the gold centers of each molecule of **9** with $Au\cdots Au$ distances of $3.0452(2)$ and $3.0307(2)$ Å. No aurophilic interactions were observed between adjacent metallomacrocycles because the closest $Au\cdots Au$ contact was over 8 Å. Crystals of **10** were grown by cooling a saturated ethyl acetate (EtOAc)/hexane solution to $25\text{ }^\circ C$ from $60\text{ }^\circ C$. **10** crystallizes in the triclinic space group $P\bar{1}$ with two molecules of **10** per unit cell along with two molecules of EtOAc. Similar to **9**, complex **10** (Figure 2) crystallized in the metallomacrocyclic form, and a comparison of the bond angles and distances between the two structures is given in Table 1.

Protodeauration Reactions. In order to probe the ability of **1** to link two metal centers, protodeauration reactions were carried out using the mononuclear precursors **2** and **3**. Stirring an acetonitrile (CH_3CN)/THF (5:1) suspension of **1** with 2 equiv of **2** or **3** cleanly generated phosphorus-metalated bimetallic complexes (**12** and **13**; Scheme 2). Monitoring the reaction of **1** with **2** in dimethyl sulfoxide ($DMSO$)- d_6 revealed a stepwise process beginning with the loss of $C_6H_5^tBu$ (1H : δ 1.27; ^-tBu) and formation of the monoaurated intermediate ($C_{12}H_9^tBu_2P^A-Au-[P^BO_3C_5H_8P^CO_3H]$). The latter was characterized by a new doublet (δ 6.97, $^1J_{HP} = 688.8$ Hz) for the unreacted $-P(O)-H$ end in the 1H NMR spectrum along with two doublets [^{31}P : δ 67.4 (d, P^A); 114.4 (d, P^B); $^2J_{P^AP^B} = 461.0$ Hz] and a singlet (δ 7.4, P^C) in the $^{31}P\{^1H\}$ NMR spectrum. It should be noted that **1** was highly soluble in $DMSO$ - d_6 , while **2** was quite insoluble (ca. <1%). Only under these substrate-starved conditions were we able to observe the reactive intermediate. Similar experiments carried out under homogeneous conditions (2:1 $DMSO$ - $d_6/CDCl_3$) yielded only signals for **12** when **1** was treated with **2**. After ca. 20% conversion into the monoaurated complex, two new doublets appeared in the ^{31}P NMR spectrum [δ 67.6 (d), 113.9 (d); $^2J_{PP} = 459.1$ Hz] and were assigned to **12** by comparison to an isolated

Scheme 1. Synthesis of Arylgold Precursors



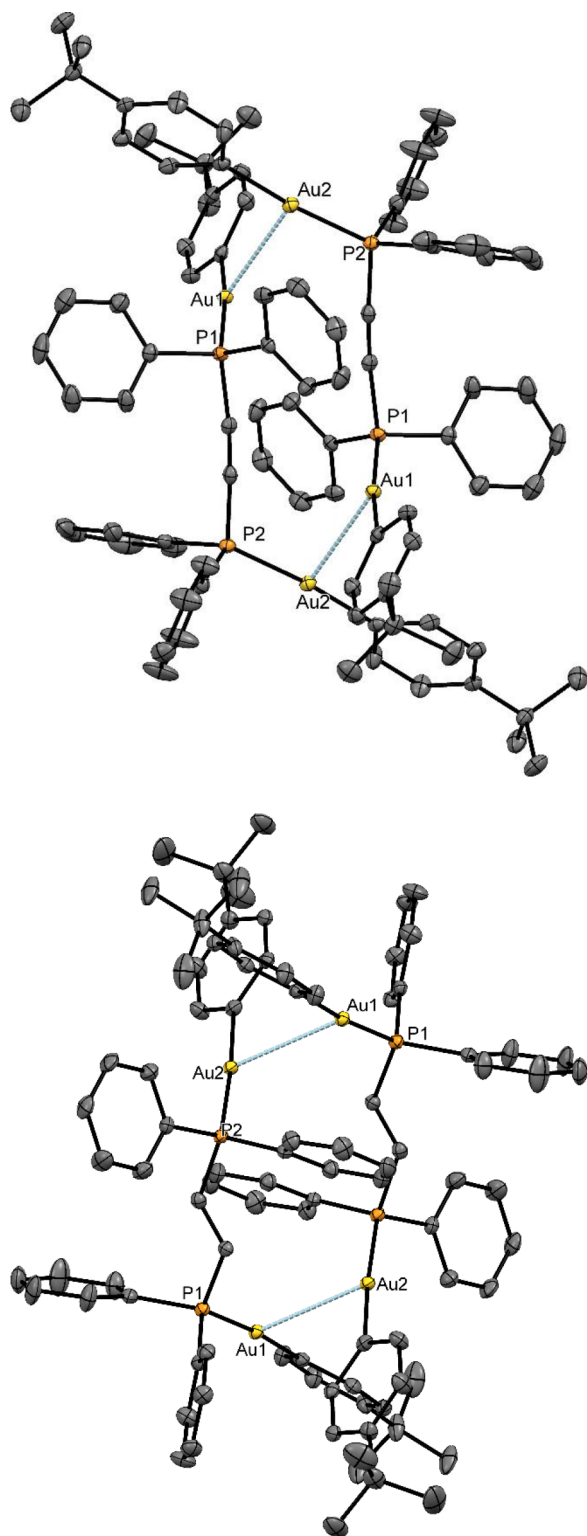


Figure 2. Structures of **9** and **10**: aggregation into 12-membered metallomacrocycles linked by auophilic interactions. Thermal ellipsoids shown at 50% probability with hydrogen atoms and EtOAc (for compound **10**) removed.

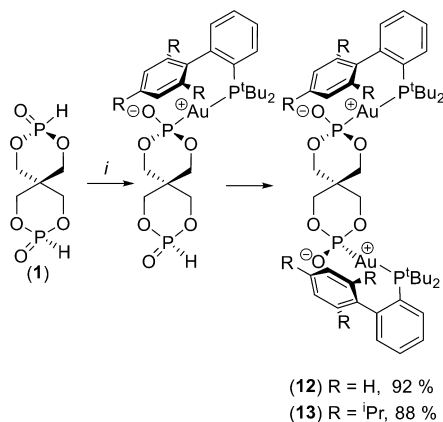
sample. Continued stirring resulted in the complete consumption of **1** and **2** and the exclusive formation of **12**.

Because of the nature of the spirocyclic linker, the attachment to gold could occur through oxygen or phosphorus. The large $^2J_{\text{PP}}$ in the $^{31}\text{P}\{^1\text{H}\}$ NMR spectra for **12** and **13**

Table 1. Selected Bond Distances (Å) and Angles (deg)

	9	10
Au...Au	3.0307(2)	3.18789(17)
Au–C _{ipso}	2.048(3), 2.044(3)	2.049(3), 2.055(3)
Au–P	2.3000(7), 2.2840(7)	2.2937(8), 2.055(3)
P–C _{≡C,C=C}	1.765(3), 1.770(3)	1.807(3), 1.808(3)
C≡C, C=C	1.207(4)	1.330(5)
P–Au–C _{≡C,C=C}	171.94(8), 174.77(8)	174.73(8), 175.51(9)
C≡C–P,C=C–P	174.6(3), 175.4(3)	124.1(2), 127.7(2)

Scheme 2. Synthesis of Bimetallic Complexes through Protodeauration^a



^a(i) LAu(C₆H₄^{*t*}Bu) (2.1 equiv), CH₃CN/THF (5:1), 16 h, 25 °C.

strongly suggest that the spirocyclic framework is attached to the gold centers through phosphorus. For these bimetallic complexes and related compounds, the [PO₃R₂][−] group can be characterized as either a *k*¹-O-anionic phosphorus(III) phosphito or a *k*¹-phosphorus(V) phosphonato donor.⁴³ Evidence for the former includes an electron localization function and natural bond orbital investigation of the bonding in related ruthenium compounds.⁴⁴ Igau and co-workers found that the oxygen had high anionic character, and the Ru–P bonding was consistent with a dative interaction. Furthermore, the ^{31}P chemical shifts of the [PO₃R₂][−] fragments from **12** and **13** are in the region (>100 ppm) typically associated with gold phosphites such as (PhO)₃PAuCl, (MeO)₃PAuCl, and [P(OH)(OR)₂]₂AuCl.^{36,45,46} As a result, the bonding description of the [PO₃R₂][−] fragment in **12** and **13** is more congruent with an L-type donor.⁴⁷

The molecular structure of **13** is shown in Figure 3 and shows that the two ^{*t*}BuXPhosAu (^{*t*}BuXPhos = 2-di-*tert*-butylphosphino-2',4',6'-triisopropylbiphenyl) fragments are located on the same side of the spirocyclic linker with an intramolecular Au–Au distance of 8.1114(3) Å. This results in the positioning of the two P–O[−] groups on the opposite side of the rigid spirocyclic framework. No auophilic interactions were found in this structure. The distance between the two phosphorus centers in the linker is 5.9413(16) Å. One of the P–Au–P angles was close to linearity [174.37(4)°], while the second deviated more significantly [166.31(4)°]. It is noteworthy that **13** crystallized as a single enantiomer in the chiral space group *P*2₁2₁1. Comparing the Au–P bond lengths from the Au–PR₃ ends with the Au–P–O[−] groups revealed that the bulky phosphine formed slightly longer [2.3229(12) and 2.3408(11) Å] bonds than the O-anionic phosphito groups [2.2989(11) and 2.3084(11) Å]. The two fused 6-membered

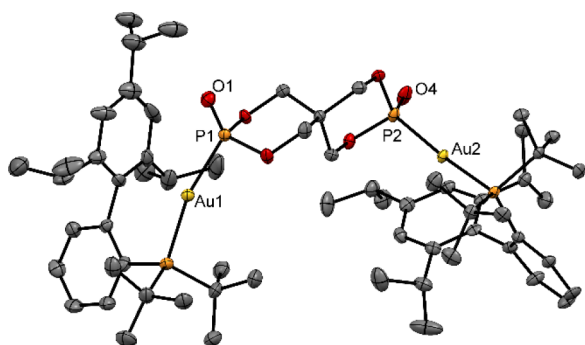


Figure 3. Molecular structure of **13**. Thermal ellipsoids shown at 50% probability with hydrogen atoms removed. Selected bond distances (Å) and bond angles (deg): Au1–P1 = 2.2989(11), Au1–P3 = 2.3229(12), Au2–P2 = 2.3084(11), Au2–P4 = 2.3408(11), P1–O1 = 1.485(4), P2–O4 = 1.475(3); P4–Au2–P2 = 174.37(4), P1–Au1–P3 = 166.31(4), Au1–P1–O1 = 126.39(14), Au2–P2–O4 = 121.30(14).

rings from the spirocyclic framework result in the generation of a twisted linker. The extent of the twist was determined by linking the two phosphorus atoms from the linker and calculating the dihedral angle [81.71(4)°] between the gold centers (Au–P–P–Au, across the linker). The angles at the ends of the linker [114.51(4)° and 108.07(3)°] were determined by calculating the P–P–Au angles (across the linker). Thus, the structure of **13** contains a twisted linker with approximately tetrahedral “corners.”

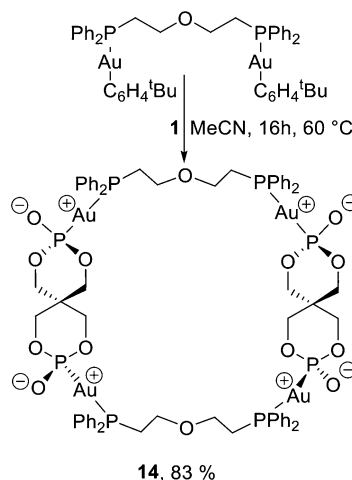
In contrast to the clean chemistry observed when **1** was treated with **2** or **3**, reactions between **1** and the diphosphine-linked diaryldigold precursors (P^AP)Au₂(C₆H₄^tBu)₂ (**4**–**11**) were considerably more complex. Stirring a solution (2.4 mM, 15:5 DMSO/THF) of **1** with (dppe)Au₂(C₆H₄^tBu)₂ [**4**; dppe = 1,2-bis(diphenylphosphino)ethane] generated an intractable mixture after stirring for 24 h at 60 °C. This mixture was highly insoluble in common solvents and only marginally soluble in DMSO. Monitoring this reaction by NMR spectroscopy (25 °C, DMSO-*d*₆) and high-resolution mass spectrometry (HRMS) revealed the formation of *tert*-butylbenzene within a few minutes of mixing along with small broad signals in the ³¹P NMR spectrum assigned to a –Ph₂P^AAuP^BO₃– fragment [δ 40.3 (d, P^A), 112.6 (d, P^B); ²J_{P^AP^B} = 497.0 Hz]. However, the dominant species observed by ³¹P NMR was the homoleptic anion {[HPO₃(C₅H₈O₃P)₂Au]}[–] [δ 127.6 (s); found *m/z* 650.9404; calcd *m/z* 650.9420] along with the chelate complex [dppe₂Au]⁺ [δ 22.5 (s); found *m/z* 993.2308; calcd *m/z* 993.2372]. Stirring this solution for 24 h resulted in the slow consumption of **1** and **4**. The broad signals at δ 40.3 and 112.6 continued to grow, although significant amounts of the [dppe₂Au]⁺ chelate as well as the {[HPO₃(C₅H₈O₃P)₂Au]}[–] anion remained after stirring. During the course of the reaction, a broad signal in the ³¹P NMR spectrum (δ 127.7) that was nearly coincident with the signal from the {[HPO₃(C₅H₈O₃P)₂Au]}[–] anion grew and was assigned to an internal (vide infra) or chain-end –{[PO₃(C₅H₈O₃P)Au–[PO₃(C₅H₈O₃P)][–] anionic fragment. Discrete species were unable to be isolated from the crude product mixture using extraction or crystallization. Similar results were obtained using the dinuclear gold precursors linked by rigid diphosphines (**8**–**10**). In the early stages of these reactions, the dominant species observed in the ³¹P NMR spectra were gold phosphito fragments along with the {[HPO₃(C₅H₈O₃P)₂Au]}[–] anion.

However, stirring for 24 h (60 °C) resulted in intractable mixtures of compounds that exhibited low solubility in all common solvents including DMSO.

In order to increase the solubility of the reaction products, analogous reactions were carried out using longer and more flexible diphosphine-linked diaryldigold precursors (**5**–**7** and **11**). Initially, these reactions gave results similar to those of **4** and **8**–**10**. As a representative example, monitoring the reaction of **1** with **6** yielded signals for the single protodeauration product [(^tBuC₆H₄)Au[P^DPh₂(CH₂)₄Ph₂P^A–Au(P^BO₃C₅H₈O₃P^CH)] [³¹P: δ 42.6 (d, P^A, ²J_{P^AP^B} = 507.2 Hz), 116.0 (d, P^B), 7.5 (s, P^C), 40.3 (s, P^D); [m + Na]⁺ found *m/z* 1203.1683; calcd *m/z* 1203.1781] within a few minutes of mixing along with the {[HPO₃(C₅H₈O₃P)₂Au]}[–] anion and the [(C₆H₄^tBu)Au(dppb)Au(dppb)Au(C₆H₄^tBu)]⁺ [dppb = 1,4-bis(diphenylphosphino)butane] cation [³¹P: δ 44.0 (s), 40.3 (s); found *m/z* 1709.4266; calcd *m/z* 1709.4364]. As the reaction proceeded, [(dppb)₂Au]⁺² (found *m/z* 623.1290; calcd *m/z* 623.1326)⁴⁸ was also identified along with a number of transient signals. Increasing the temperature to 60 °C and stirring for 16 h consumed **1** and **6**, as well as all of the charged and transient species. The reaction mixture displayed higher solubility in DMSO and exhibited a single set of broad signals in the ³¹P NMR spectrum (δ 115.1 and 42.7; ²J_{PP} = 506 Hz). While this suggested that the product could be an oligomer/polymer or framework, we were unable to find end groups in the ³¹P or ¹H NMR spectra. If the molecular weight of the material was high, clearly identifying end groups would be challenging. Alternatively, the product could be cyclic. Working under this premise, analysis of the crude reaction mixture revealed the 30-membered metallomacrocyclic,⁴⁹ dppb₂Au₄[PO₃(C₅H₈O₃P)₂] ([m + H]⁺ found *m/z* 2093.1609; calcd *m/z* 2093.1661). However, the crude reaction mixture was still highly insoluble and contained several reaction products that were unable to be separated.

The reaction between **1** and **11** initially mirrored these results. However, in contrast to the reactions of **1** with **4**–**10**, two sharp doublets were observed in the ³¹P NMR spectrum [δ 111.0 (d), 37.5 (d); ²J_{PP} = 519.7 Hz] after heating (16 h, 60 °C). The product from this reaction was identified as the 32-membered metallomacrocyclic {[Ph₂P–(CH₂)₂O]₂Au₄[PO₃(C₅H₈O₃P)₂] (**14**, Scheme 3; ([m +

Scheme 3. Synthesis of a Metallomacrocyclic through Protodeauration/Cyclization



H]⁺ found m/z 2125.1477; calcd m/z 2125.1559). It should be noted that we cannot distinguish between a closed macrocycle where the fragments are in similar magnetic environments and a dynamic system characterized by rapid cleavage/reassembly. In contrast to the other reaction products, **14** was soluble in chloroform as well as boiling CH₃CN. No dynamic behavior was observed in the ¹H or ³¹P NMR spectra between −40 and +65 °C (CDCl₃). It was noteworthy that the formation of **14** was relatively insensitive to the concentration of the protodeauration/cyclization reaction. Increasing the concentration of the reaction by a factor of 4 to promote the formation of oligomers/polymers still resulted in the sole formation of **14**.

While **14** could be readily crystallized from CH₃CN, the crystals were extremely fragile. Fortunately, diffusion of EtOAc into a saturated DMSO solution of **14** afforded single crystals that were suitable for X-ray diffraction (Figure 4). Instead of

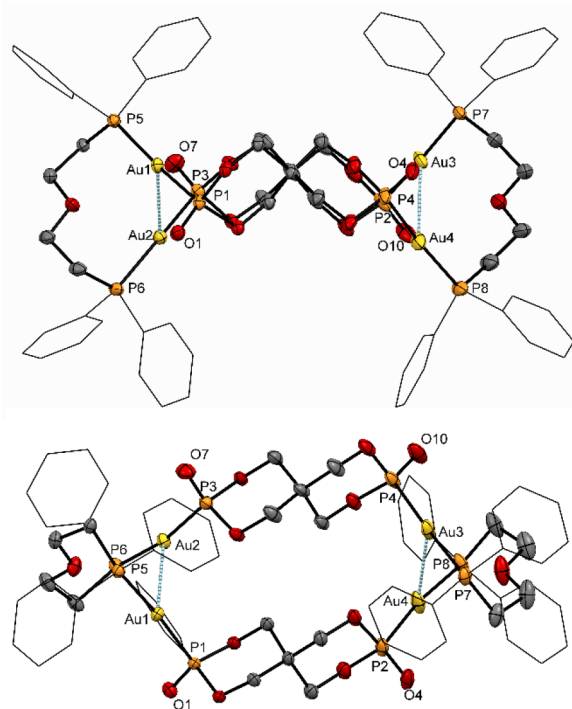


Figure 4. Structure of **14**: rotated views. Thermal ellipsoids at 30% probability and hydrogen atoms omitted. Selected bond distances (Å) and angles (deg): Au1–P1 = 2.3034(18), Au1–P5 = 2.3446(19), Au2–P3 = 2.2960(19), Au2–P6 = 2.3375(19), Au3–P4 = 2.293(2), Au3–P7 = 2.322(2), Au4–P2 = 2.288(2), Au4–P8 = 2.322(2), P1–O1 = 1.482(5), P2–O4 = 1.484(6), P3–O7 = 1.493(6), P4–O10 = 1.478(6); Au1–P1–O1 = 117.9(2), Au2–P3–O7 = 119.3(3), Au3–P4–O10 = 118.7(3), Au4–P2–O4 = 117.2(2), P1–Au1–P5 = 172.39(7), P3–Au2–P6 = 168.78(7), P4–Au3–P7 = 175.68(9), P2–Au4–P8 = 171.88(10).

the open/expanded system shown in Scheme 3, the cavity of the metallomacrocycle is compressed and held together by two aurophilic interactions [3.1699(5) and 3.4936(7) Å]. The flexibility of the [Ph₂P(CH₂)₂]₂O linker accommodates these aurophilic interactions and twists to bring the spirocyclic components together and facilitate the metal–metal interactions. The shortest Au–Au contact across the cavity of the metallomacrocycle is 8.1910(6) Å. Similar to the structure of **13**, the P–P distances across each side are 5.897(3) and 5.889(3) Å, while the torsion angles (Au–P–P–Au, each side

of the tetramer) were 84.87(8) and 85.22(8)°. The angles at the phosphorus corners (P–P–Au) are between 110.49(7) and 125.81(7)°.

These results from the mechanistic studies are consistent with the process shown in Scheme 4. The initial protodeauration between **1** and **4**–**11** generated the monoaurated intermediate. This species underwent reversible ligand redistribution to generate the homoleptic anion and cation {[HPO₃(C₅H₈)O₃P]₂Au}[−] and [ArAu(P[^]P)Au(P[^]P)AuAr]⁺. Similar reactions have been reported for mononuclear systems.³⁶ These ligand-exchange processes were not observed in the reactions of **1** with **2** or **3** because of the steric bulk of the dialkylbiarylphosphine ligands.³⁴ Further redistribution generated a (P[^]P)₂Au⁺ chelate or (P[^]P)₂Au₂⁺² bridged bimetallic complex/oligomers depending on the length and flexibility of the diphosphine. Indeed, significant amounts of (dppe)₂Au⁺ were observed in the reaction between **1** and **4** because of the stability of the 5-membered chelate. For reactions involving rigid and shorter diphosphines, these redistribution products persisted for the duration of the reaction, while reactions involving longer and more flexible diphosphines (**5**–**7** and **11**) consumed these charged species. It is worth noting that, once the metallomacrocycle was generated, no reversible ligand redistribution was observed. Both the solution and solid-state structures of diphosphine-linked gold compounds can be challenging to predict. There can be a dependence on the overall length as well as the number of methylene groups (even or odd) in the tether between the diphenylphosphino fragments.⁵⁰ In some cases, shorter tethers between the diphenylphosphino fragments results in the formation of discrete species, while longer tethers generate oligomers as well as equilibrium mixtures of cyclic and acyclic products.⁴¹ Because of the higher solubility of **14**, our remaining efforts focused on the chemistry of this metallomacrocycle.

Over the past few decades, there has been considerable interest in developing new types of phosphorus-containing macrocycles because of their applications in mechanically interlocked molecules and molecular machines.^{51–54} Additionally, there has been growing interest in the use of macrocycles to modify the activity of chemotherapeutic agents.⁵⁵ Recent examples include using pillar[*n*]arenes to enhance variations of photodynamic therapy⁵⁶ as well as to increase the solubility and efficacy of tamoxifen.⁵⁷ For breast cancer, managing the effects of β-estradiol (estrogen) and estrogenic materials is a critical concern for estrogen-receptor-positive breast cancer. Given the size and flexibility of the 32-membered metallomacrocycle (**14**) as well as the presence of eight oxygen atoms on the interior, **14** could interact with estrogen. This possibility was investigated using ¹H and ³¹P NMR spectroscopy. The treatment of **14** (4.7 mM, dry and deacidified CDCl₃) with estradiol (E₂, 1 equiv) resulted in significant changes in the chemical shifts of several hydrogen atoms from estradiol. It should be noted that estradiol was quite insoluble in dry (deacidified) CDCl₃; however, the solution of **14** with estradiol was completely homogeneous, suggesting that the metallomacrocycle aids in solubilization of the estradiol. The low solubility of estradiol also complicated our attempts to determine the stoichiometry of the host–guest complex. The hydrogen atom most affected by the addition of **14** was 3-OH (Figure 5). Its resonance moves from 4.56 ppm in the free state to 8.00 ppm (Δδ = 3.44 ppm) in the presence of **14**. Additionally, the signals for the A-ring hydrogen atoms shifted

Scheme 4. Ligand Redistribution Reactions Observed in the Protodeauration/Cyclization Reactions

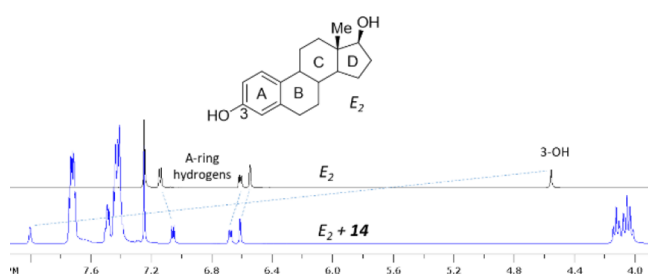
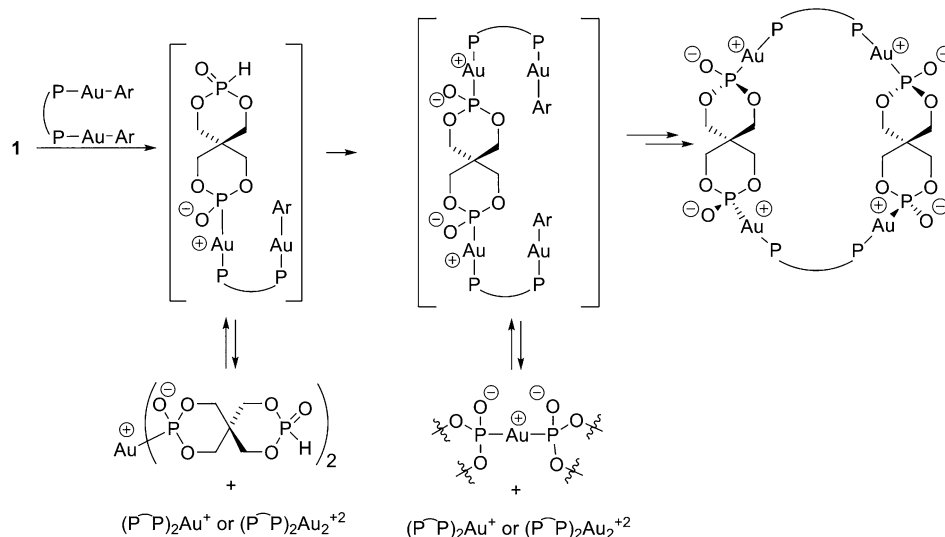


Figure 5. Interaction between the metallomacrocyclic complex **14** and estradiol (25 °C, CDCl₃).

closer together relative to free estradiol. Only minor changes were observed in the ¹H and ³¹P NMR spectra for **14** when estradiol was added. The shifting of 3-OH is likely due to hydrogen bonding with the oxygen atom from the Au–P–O[−] group.^{54,58,59} Additionally, the shifting of the A-ring hydrogen atoms could be an indication that the ring was close enough for an interaction with the gold center.^{60–63} Although **14** could be readily characterized by HRMS, the estrogen adduct did not survive the electrospray conditions. With the exception of 3-OH, no significant changes were observed from either **14** or estradiol upon cooling of this solution to −40 °C (see the [Supporting Information](#)). Only 3-OH moved as the temperature was lowered because of the known dependence of hydrogen bonding on the temperature.⁶⁴ The ability of **14** to interact with testosterone was also screened. The treatment of **14** with testosterone (1 equiv) resulted in very minor changes in the chemical shifts and coupling constants of the hydrogen atoms from **14** and testosterone.

CONCLUSIONS

This work demonstrated that a spirocyclic diphosphite can successfully be used for the preparation of bimetallic complexes through protodeauration and metallomacrocycles through a protodeauration/cyclization process. A mechanistic investigation revealed that the gold phosphito intermediates undergo a series of reversible ligand redistribution reactions to generate charged species. Depending on the size and geometry of the tether linking the diphenylphosphino groups together, these charged species either persisted or were consumed to

generate metallomacrocycles. Once the metallomacrocyclic was generated, no ligand redistribution was observed. These redistribution reactions could also be circumvented through the use of bulky phosphine ligands. It is possible that the observed ligand redistribution reactions are specific to gold, and future work will answer the question of whether or not other metal phosphito complexes undergo similar processes. In the X-ray structure of a 32-membered metallomacrocyclic, the cavity was compressed because of the twisting of the compound in order to accommodate two aurophilic interactions. Metallomacrocyclic **14** provides a flexible framework that can bend and twist to accommodate guest molecules. Additional binding/recognition studies using **14** and related compounds are ongoing and will be reported in due course.

EXPERIMENTAL SECTION

General Considerations. All solvents were dried using a Grubbs-type solvent purification system and distilled prior to use with the exception of CH₃CN (CaH₂) and DMSO (3 Å sieves). The chlorogold precursors (P[^]P)Au₂Cl₂ were generated by the displacement of dimethyl sulfide from (Me₂S)AuCl using 0.5 equiv of the diphosphine in CH₂Cl₂.^{65–70} The mononuclear precursors [^tBuXPhosAu(C₆H₄^tBu) and JohnPhosAu(C₆H₄^tBu)] (JohnPhos = 2-biphenyldi-*tert*-butylphosphine) were generated following literature procedures.⁷¹ **1** was generated by a modification of the literature procedure as described below.²¹ DMSO-*d*₆ was dried over activated molecular sieves (3 Å). CDCl₃ was dried over CaH₂ and distilled immediately prior to use. ¹H NMR chemical shifts were determined by reference to residual nondeuterated solvent resonances, and ¹³C{¹H} chemical shifts were determined by reference to deuterated solvent resonances. Coupling constants are given in hertz. ³¹P{¹H} NMR spectra were referenced to external H₃PO₄ (0 ppm). Standard flash silica gel [60 Å, treated with triethylamine (NEt₃)] was used for the chromatographic isolation of arylgold compounds. Silica (thin-layer chromatography) plates were rinsed with NEt₃ solutions and dried immediately prior to use. The connectivity and individual peak assignments were determined through analysis of standard 1D experiments along with heteronuclear single quantum coherence, attached proton test, and correlation NMR spectra. ABX systems were modeled using Spinworks. Elemental analyses were determined by Midwest Microlabs. HRMS data were obtained on a Thermo Scientific Exactive Plus liquid chromatography/mass spectrometry system (electrospray ionization, ESI).

Preparation of 2,4,8,10-Tetraoxa-3,9-diphosphaspiro[5.5]-undecane 3,9-Dioxide (1**).** The title compound was made by a

modification of the literature procedure.²¹ A round-bottom flask was charged with pentaerythritol (1.00 g, 7.34 mmol) and a magnetic stirring bar. After the flask was sealed with a septum and the atmosphere was exchanged with nitrogen, diphenyl phosphite (3.00 mL, 15.7 mmol) and pyridine (10 mL) were added by syringe. The mixture was stirred for 2 h, followed by the injection of dichloromethane (60 mL). A white solid formed and was triturated by vigorous stirring for 20 min. The solid was collected by filtration and triturated a second time with dichloromethane (60 mL). The solid was collected on a glass frit, washed with dichloromethane (50 mL), and dried under vacuum to afford **1** as a free-flowing powder (1.03 g, 62%).

Preparation of $\text{LAu}_2(\text{C}_6\text{H}_4^t\text{Bu})_2$ Precursors. General Procedure A. A vial (30 mL) was charged in air with the LAu_2Cl_2 precursor (1 equiv), Cs_2CO_3 (4 equiv), 4-*tert*-butylphenylboronic acid (4 equiv), and a magnetic stirring bar. The atmosphere was exchanged for nitrogen using a vacuum manifold, and 15 mL of isopropyl alcohol (reagent grade) was injected by syringe. After stirring at 50 °C for 16 h in a block heater, the reaction mixture was concentrated and dried under vacuum for 24 h. The residue was triturated with 10 mL of methanol for 2 h. The insoluble material was separated using a centrifuge and was subsequently triturated with THF (30 mL) or dichloromethane (30 mL) for 1 h and filtered through Celite. The volatiles were removed under vacuum, and the crude product was purified by column chromatography. Because of the potential for decomposition of the arylgold compound, the silica gel was stirred with 10% NEt_3 in EtOAc for 30 min, loaded onto the column, and flushed with eluent (3 times the column volume) immediately prior to use.

Preparation of $(\text{dppe})\text{Au}_2(\text{C}_6\text{H}_4^t\text{Bu})_2$ (4**).** General procedure A was followed using $(\text{dppe})\text{Au}_2\text{Cl}_2$ (1.000 g, 1.158 mmol), Cs_2CO_3 (1.570 g, 4.665 mmol), and 4-*tert*-butylphenylboronic acid (0.830 g, 4.66 mmol). Chromatography details: 61 g of NEt_3 -treated silica gel, hexane/EtOAc (gradient: 100:0–0:100), R_f = 0.40 (3:1 hexane/EtOAc). After drying over MgSO_4 , the suspension was filtered, and the volatiles were removed to afford the title compound as a white solid (0.873 g, 71%). Anal. Calcd for $\text{C}_{46}\text{H}_{50}\text{Au}_2\text{P}_2$: C, 52.18; H, 4.76. Found: C, 52.02; H, 4.70. ^1H NMR (CDCl_3 , 25 °C): δ 7.75 (m, 8H, Ar–H), 7.55 (m, 4H, Ar–H), 7.48 (m, 12H, Ar–H), 7.38 (d, 4H, J = 7.7, Ar–H), 2.76 (br s, 4H, $-\text{CH}_2-$), 1.33 (s, 18H, $-\text{CH}_3$). $^{13}\text{C}\{^1\text{H}\}$ NMR (CDCl_3 , 25 °C): δ 169.8 (X part of an ABX pattern, $^2J_{\text{CP}}$ = 118.2, $^3J_{\text{CP}}$ = 52.4, $\Delta\delta$ = 0.8 ppm, quat), 148.7 (s, quat), 139.1 (s, $-\text{CH}$), 133.7 (app t, J = 6.8, $-\text{CH}$), 131.7 (s, $-\text{CH}$), 130.9 (X part of an ABX pattern, $^1J_{\text{CP}}$ = 45.4, $^4J_{\text{CP}}$ = 1.5, $^3J_{\text{PP}}$ = 52.8, $\Delta\delta$ = 2.4 ppm, quat), 129.5 (app t, J = 5.2, $-\text{CH}$), 124.8 (br s, $-\text{CH}$), 34.5 (s, quat), 31.6 (s, $-\text{CH}_3$), 24.1 (br t, J = 17.4, $-\text{CH}_2-$). $^{31}\text{P}\{^1\text{H}\}$ NMR (CDCl_3 , 25 °C): δ 42.0 (s).

Preparation of $(\text{dppp})\text{Au}_2(\text{C}_6\text{H}_4^t\text{Bu})_2$ (5**; dppp = 1,3-Bis-(diphenylphosphino)propane).** General procedure A was followed using $(\text{dppp})\text{Au}_2\text{Cl}_2$ (1.000 g, 1.140 mmol), Cs_2CO_3 (1.492 g, 4.580 mmol), and 4-*tert*-butylphenylboronic acid (0.812 g, 4.56 mmol). Chromatography details: 55 g of NEt_3 -treated silica gel, hexane/EtOAc (gradient 100:0–80:20), R_f = 0.45 (3:1 hexane/EtOAc). After drying over MgSO_4 , the suspension was filtered, and the volatiles were removed to afford the title compound as a white solid (0.960 g, 79%). Anal. Calcd for $\text{C}_{47}\text{H}_{52}\text{Au}_2\text{P}_2$: C, 52.62; H, 4.89. Found: C, 52.68; H, 4.91. ^1H NMR (CDCl_3 , 25 °C): δ 7.72 (dd, 8H, J = 11.5, 7.7, ArH), 7.48 (m, 4H, ArH), 7.42 (t, 4H, J = 7.5, ArH), 7.35 (t, 8H, J = 7.5, ArH), 7.28 (d, 4H, J = 7.9, ArH), 2.94 (m, 4H, $-\text{CH}_2-$), 1.98 (m, 2H, $-\text{CH}_2-$), 1.31 (s, 18H, $-\text{CH}_3$). $^{13}\text{C}\{^1\text{H}\}$ NMR (CDCl_3 , 25 °C): δ 169.3 (d, J = 117.3, quat), 148.3 (s, quat), 139.4 (s, ArCH), 133.8 (d, J = 13.3, ArCH), 131.6 (d, J = 46.7, quat), 131.3 (s, ArCH), 129.2 (d, J = 10.4, ArCH), 124.6 (d, J = 5.9, ArCH), 34.5 (s, quat), 31.7 (s, $-\text{CH}_3$), 29.1 (dd, J = 29.1, 10.4, $-\text{CH}_2-$), 20.1 (t, J = 4.4, $-\text{CH}_2-$). $^{31}\text{P}\{^1\text{H}\}$ NMR (CDCl_3 , 25 °C): δ 36.7 (s).

Preparation of $(\text{dppb})\text{Au}_2(\text{C}_6\text{H}_4^t\text{Bu})_2$ (6**).** General procedure A was followed using $(\text{dppb})\text{Au}_2\text{Cl}_2$ (1.000 g, 1.122 mmol), Cs_2CO_3 (1.462 g, 4.487 mmol), and 4-*tert*-butylphenylboronic acid (0.799 g, 4.49 mmol). Chromatography details: 57 g of NEt_3 -treated silica gel, hexane/EtOAc (gradient 100:0–80:20), R_f = 0.55 (3:1 hexane/

EtOAc). After drying over MgSO_4 , the suspension was filtered, and the volatiles were removed to afford the title compound as a white solid (0.993 g, 81%). Anal. Calcd for $\text{C}_{48}\text{H}_{54}\text{Au}_2\text{P}_2$: C, 53.05; H, 5.01. Found: C, 53.07; H, 4.93. ^1H NMR (CDCl_3 , 25 °C): δ 7.69 (dd, 8H, J = 11.5, 7.5, ArH), 7.49 (m, 4H, ArH), 7.42 (m, 12H, ArH), 7.32 (d, 4H, J = 7.5, ArH), 2.41 (m, 4H, $-\text{CH}_2-$), 1.85 (m, 4H, $-\text{CH}_2-$). 1.30 (s, 18H, $-\text{CH}_3$). $^{13}\text{C}\{^1\text{H}\}$ NMR (CDCl_3 , 25 °C): δ 169.9 (d, J = 117.7, quat), 148.5 (s, quat), 139.2 (s, ArCH), 133.6 (d, J = 13.3, ArCH), 132.1 (d, J = 46.4, quat), 131.3 (s, ArCH), 129.3 (d, J = 10.6, ArCH), 124.7 (d, J = 6.4, ArCH), 34.5 (s, quat), 31.6 (s, $-\text{CH}_3$), 28.1 (d, J = 29.7, $-\text{CH}_2-$), 27.2 (dd, J = 16.5, 5.5, $-\text{CH}_2-$). $^{31}\text{P}\{^1\text{H}\}$ NMR (CDCl_3 , 25 °C): δ 39.2 (s).

Preparation of $(\text{dpppent})\text{Au}_2(\text{C}_6\text{H}_4^t\text{Bu})_2$ (7**; dpppent = 1,5-Bis(diphenylphosphino)pentane).** General procedure A was followed using $(\text{dpppent})\text{Au}_2\text{Cl}_2$ (1.000 g, 1.105 mmol), Cs_2CO_3 (1.440 g, 4.420 mmol), and 4-*tert*-butylphenylboronic acid (0.787 g, 4.42 mmol). Chromatography details: 45 g of NEt_3 -treated silica gel, hexane/EtOAc (gradient 100:0–80:20), R_f = 0.48 (2:1 hexane/EtOAc). After drying over MgSO_4 , the suspension was filtered, and the volatiles were removed to afford the title compound as a white solid (0.874 g, 85%). Anal. Calcd for $\text{C}_{49}\text{H}_{56}\text{Au}_2\text{P}_2$: C, 53.46; H, 5.13. Found: C, 53.49; H, 5.18. ^1H NMR (CDCl_3 , 25 °C): δ 7.70 (m, 8H, ArH), 7.49 (m, 4H, ArH), 7.42 (m, 12H, ArH), 7.30 (d, 4H, J = 7.9, ArH), 2.37 (m, 4H, $-\text{CH}_2-$), 1.72 (m, 6H, $-\text{CH}_2-$), 1.29 (s, 18H, $-\text{CH}_3$). $^{13}\text{C}\{^1\text{H}\}$ NMR (CDCl_3 , 25 °C): δ 169.9 (d, J = 117.2, quat), 148.4 (s, quat), 139.2 (s, ArCH), 133.6 (d, J = 13.0, ArCH), 132.3 (d, J = 46.4, quat), 131.2 (s, ArCH), 129.2 (d, J = 10.2, ArCH), 124.7 (d, J = 3.9, ArCH), 34.5 (s, quat), 32.0 (t, J = 14.5, $-\text{CH}_2-$), 31.7 (s, $-\text{CH}_3$), 27.7 (d, J = 29.7, $-\text{CH}_2-$), 24.8 (d, J = 4.7, $-\text{CH}_2-$). $^{31}\text{P}\{^1\text{H}\}$ NMR (CDCl_3 , 25 °C): δ 39.1 (s).

Preparation of $(\text{dpephos})\text{Au}_2(\text{C}_6\text{H}_4^t\text{Bu})_2$ (8**; DPEphos = (Oxydi-2,1-phenylene)bis(diphenylphosphine)).** General procedure A was followed using $(\text{DPEphos})\text{Au}_2\text{Cl}_2$ (1.000 g, 0.997 mmol), Cs_2CO_3 (1.299 g, 3.987 mmol), and 4-*tert*-butylphenylboronic acid (0.710 g, 3.99 mmol). Chromatography details: 70 g of NEt_3 -treated silica gel, hexane/EtOAc (gradient 100:0–80:20), R_f = 0.34 (3:1 hexane/EtOAc). After drying over MgSO_4 , the suspension was filtered, and the volatiles were removed to afford the title compound as a white solid (0.882 g, 74%). Anal. Calcd for $\text{C}_{56}\text{H}_{54}\text{Au}_2\text{OP}_2$: C, 56.10; H, 4.54. Found: C, 55.85; H, 4.61. ^1H NMR (CDCl_3 , 25 °C): δ 7.53 (dd, 4H, J = 11.5, 7.7, Ar–H), 7.46 (m, 4H, ArH), 7.39 (m, 4H, ArH), 7.21–7.07 (m, 22H, ArH), 6.78 (ddd, 2H, J = 13.5, 7.8, 1.9, ArH), 1.26 (s, 18H, $-\text{CH}_3$). $^{13}\text{C}\{^1\text{H}\}$ NMR (CDCl_3 , 25 °C): δ 168.5 (d, J = 120.3, quat), 160.3 (d, J = 7.2, quat), 147.8 (s, quat), 139.1 (s, ArCH), 135.6 (d, J = 14.1, ArCH), 134.6 (d, J = 4.2, ArCH), 133.6 (d, J = 13.8, ArCH), 133.5 (s, ArCH), 131.2 (d, J = 49.3, quat), 131.3 (d, J = 2.2, ArCH), 130.2 (d, J = 2.4, ArCH), 129.8 (d, J = 50.7, quat), 129.1 (d, J = 10.7, ArCH), 124.7 (d, J = 7.4, ArCH), 124.3 (d, J = 5.4, ArCH), 122.2 (d, J = 47.2, quat), 120.9 (d, J = 4.5, ArCH), 34.4 (s, quat), 31.7 (s, $-\text{CH}_3$). $^{31}\text{P}\{^1\text{H}\}$ NMR (CDCl_3 , 25 °C): δ 37.3 (s).

Preparation of $(\text{dppa})\text{Au}_2(\text{C}_6\text{H}_4^t\text{Bu})_2$ (9**; dppa = 1,2-Bis-(diphenylphosphino)acetylene).** General procedure A was followed using $(\text{dppa})\text{Au}_2\text{Cl}_2$ (1.000 g, 1.164 mmol), Cs_2CO_3 (1.517 g, 4.656 mmol), and 4-*tert*-butylphenylboronic acid (0.829 g, 4.66 mmol). Chromatography details: 30 g of NEt_3 -treated silica gel, hexane/EtOAc (gradient 100:0–80:20), R_f = 0.26 (3:1 hexane/EtOAc). After drying over MgSO_4 , the suspension was filtered, and the volatiles were removed to afford the title compound as a white solid (0.948 g, 77%). X-ray-quality crystals were grown by cooling a THF/ CH_2Cl_2 solution. A sample of **9** (0.500 g) was suspended in THF (5 mL), and CH_2Cl_2 (~20 mL) was added until a homogeneous solution was obtained. The solution was filtered through Celite, placed in a scratched sample vial (27 mL), and sealed with a Teflon-lined crimp cap. The vial was allowed to stand undisturbed for 5 days (–10 °C). Colorless crystals of **9** were separated by filtration and dried under vacuum (0.36 g, 72%). Anal. Calcd for $\text{C}_{46}\text{H}_{46}\text{Au}_2\text{P}_2$: C, 52.38; H, 4.40. Found: C, 52.56; H, 4.12. ^1H NMR (CDCl_3 , 25 °C): δ 7.84 (dd, 8H, J = 13.4, 7.6, ArH), 7.48 (m, 16H, ArH), 7.32 (d, 4H, J = 7.6, ArH), 1.30 (s, 18H, $-\text{CH}_3$). $^{13}\text{C}\{^1\text{H}\}$ NMR (CDCl_3 , 25 °C): δ 166.6 (d, J = 122.3, quat), 149.0 (s, quat), 139.1 (s, ArCH), 133.7 (d, J = 15.8, ArCH),

132.2 (d, $J = 2.1$, ArCH), 129.7 (d, $J = 55.5$, quat), 129.6 (d, $J = 11.9$, ArCH), 124.8 (d, $J = 6.6$, ArCH), 102.7 (dd, $J = 68.8$, 6.1, $\equiv\text{C}-$), 34.6 (s, quat), 31.6 (s, $-\text{CH}_3$). $^{31}\text{P}\{^1\text{H}\}$ NMR (CDCl_3 , 25 °C): δ 21.1 (s).

Preparation of $(\text{dppee})\text{Au}_2(\text{C}_6\text{H}_4^t\text{Bu})_2$ [10; dppee = (*E*)-1,2-Bis(diphenylphosphino)ethane]. General procedure A was followed using $(\text{dppee})\text{Au}_2\text{Cl}_2$ (1.000 g, 1.161 mmol), Cs_2CO_3 (1.513 g, 4.644 mmol), and 4-*tert*-butylphenylboronic acid (0.827 g, 4.65 mmol). Chromatography details: 50 g of NEt_3 -treated silica gel, hexane/EtOAc (gradient 100:0–80:20), $R_f = 0.31$ (3:1 hexane/EtOAc). After drying over MgSO_4 , the suspension was filtered, and the volatiles were removed to afford the title compound as a white solid (0.801 g, 65%). Anal. Calcd for $\text{C}_{46}\text{H}_{48}\text{Au}_2\text{P}_2$: C, 52.28; H, 4.58. Found: C, 52.40; H, 4.37. X-ray-quality crystals were grown by cooling an EtOAc/hexane solution. A sample of **10** (0.500 g) and a microstirring bar were added to a 27 mL scratched sample vial and sealed with a Teflon-lined crimp cap. While the mixture was heated (60 °C) and stirred, EtOAc was added by syringe until the compound was fully dissolved (~2 mL). With continued heating, hexane (~20 mL) was added by syringe. The heated vial was cooled to 25 °C and allowed to stand undisturbed for 72 h. The colorless crystals were separated by filtration and dried under vacuum (0.41 g, 82%). ^1H NMR (CDCl_3 , 25 °C): δ 7.67 (m, 8H, Ar–H), 7.48 (m, 16H, Ar–H), 7.37 (t, 2H, $J = 17.9$, $=\text{CH}$), 7.32 (m, 4H, Ar–H), 1.29 (s, 18H, $-\text{CH}_3$). $^{13}\text{C}\{^1\text{H}\}$ NMR (CDCl_3 , 25 °C): δ 168.4 (X part of an ABX pattern, $^2J_{\text{CP}} = 117.9$, $^3J_{\text{PP}} = 38.0$, $^3J_{\text{CP}} = 0$, $\Delta\delta = 0.7$ Hz, quat), 148.6 (s, quat), 142.4 (X part of an ABX pattern, $^1J_{\text{CP}} = 36.7$, $^3J_{\text{PP}} = 38.0$, $^2J_{\text{CP}} = 7.5$, $\Delta\delta = 4.7$ Hz, $=\text{CH}$), 138.8 (s, ArCH), 133.9 (app t, $J = 7.0$, ArCH), 131.7 (s, ArCH), 130.0 (X part of an ABX pattern, $^1J_{\text{CP}} = 49.4$, $^3J_{\text{PP}} = 38.0$, $^4J_{\text{CP}} = 0$, $\Delta\delta = 2.5$ Hz, $=\text{CH}$), 129.4 (app t, $J = 5.4$, ArCH), 124.5 (app t, $J = 3.0$, ArCH), 34.3 (s, quat), 31.4 (s, $-\text{CH}_3$). $^{31}\text{P}\{^1\text{H}\}$ NMR (CDCl_3 , 25 °C): δ 39.1 (s).

Preparation of $(\text{Ph}_2\text{P}(\text{CH}_2)_2\text{O}(\text{CH}_2)_2\text{PPh}_2)\text{Au}_2(\text{C}_6\text{H}_4^t\text{Bu})_2$ (11). General procedure A was followed using $(\text{Ph}_2\text{P}(\text{CH}_2)_2\text{O}(\text{CH}_2)_2\text{PPh}_2)\text{Au}_2\text{Cl}_2$ (1.000 g, 1.102 mmol), Cs_2CO_3 (1.436 g, 4.407 mmol), and 4-*tert*-butylphenylboronic acid (0.785 g, 4.41 mmol). Chromatography details: 51 g of NEt_3 -treated silica gel, hexane/EtOAc (gradient 100:0–50:50), $R_f = 0.54$ (2:1 hexane/EtOAc). After drying (MgSO_4), the suspension was filtered, and the volatiles removed to afford the title compound as a white solid (0.827 g, 68%). Anal. Calcd for $\text{C}_{48}\text{H}_{54}\text{Au}_2\text{OP}_2$: C, 52.28; H, 4.94. Found: C, 52.57; H, 5.11. ^1H NMR (CDCl_3 , 25 °C): δ 7.69 (dd, 8H, $J = 11.3$, 7.5, ArH), 7.50 (m, 4H, ArH), 7.45–7.38 (m, 12H, ArH), 7.30 (d, 4H, $J = 7.3$, ArH), 3.77 (dt, 4H, $J = 12.1$, 7.1, $-\text{CH}_2-$), 2.71 (dt, 4H, $J = 9.7$, 7.0, $-\text{CH}_2-$), 1.29 (s, 18H, $-\text{CH}_3$). $^{13}\text{C}\{^1\text{H}\}$ NMR (CDCl_3 , 25 °C): δ 169.6 (d, $J = 118.5$, quat), 148.4 (s, quat), 139.2 (s, ArCH), 133.7 (d, $J = 13.5$, ArCH), 132.1 (d, $J = 47.3$, quat), 131.2 (d, $J = 2.2$, ArCH), 129.2 (d, $J = 10.6$, ArCH), 124.7 (d, $J = 6.3$, ArCH), 66.9 (d, $J = 9.9$, $-\text{CH}_2-$), 34.5 (s, quat), 31.7 (s, $-\text{CH}_3$), 29.1 (d, $J = 29.7$, $-\text{CH}_2-$). $^{31}\text{P}\{^1\text{H}\}$ NMR (CDCl_3 , 25 °C): δ 34.6 (s).

Preparation of Bimetallic Complexes: General Procedure B. A vial (10 mL) was charged in air with $\text{LAuCl}_4^t\text{Bu}$ (2.1 equiv), **1** (1 equiv), and a magnetic stirring bar. The atmosphere was exchanged for nitrogen using a manifold. CH_3CN (6 mL) and THF (1 mL) were injected by syringe, and the resulting suspension was stirred at 25 °C for 16 h. The bimetallic complexes were separated by extraction/precipitation as described in the following sections.

Preparation of $[\text{JohnPhosAu}]_2[\text{PO}_3\text{C}_5\text{H}_8\text{O}_3\text{P}]$ (12). General method B was followed using $[\text{JohnPhosAu}]\text{C}_6\text{H}_4^t\text{Bu}$ (0.200 g, 0.318 mmol) and **1** (0.034 g, 0.15 mmol). The crude reaction mixture was centrifuged, and the CH_3CN /THF solution was discarded. The solid was extracted with THF (5 mL \times 2) and dried under vacuum to afford 0.167 g (92%) of a white powder. HRMS ESI. Calcd for $\text{C}_{45}\text{H}_{63}\text{Au}_2\text{O}_6\text{P}_4$ [(M + H) $^+$]: m/z 1217.2902. Found: m/z 1217.2873. Anal. Calcd for $\text{C}_{45}\text{H}_{62}\text{Au}_2\text{O}_6\text{P}_4$: C, 44.42; H, 5.14. Found: C, 44.39; H, 5.35. ^1H NMR (CDCl_3 , 25 °C): δ 7.82 (t, 2H, $J = 7.1$, ArH), 7.55–7.42 (m, 10H, ArH), 7.24 (m, 2H, ArH), 7.14 (m, 4H, ArH), 4.14 (dd, 2H, $J = 17.0$, 11.5, $-\text{CH}_2-$), 4.05 (dd, 2H, $J = 15.4$, 11.5, $-\text{CH}_2-$), 3.77 (t, 2H, $J = 11.4$, $-\text{CH}_2-$), 3.71 (t, 2H, $J = 11.5$, $-\text{CH}_2-$), 1.39 (d, 18H, $J = 15.1$, $-\text{CH}_3$), 1.38 (d, 18H, $J = 15.1$,

$-\text{CH}_3$). $^{13}\text{C}\{^1\text{H}\}$ NMR (CDCl_3 , 25 °C): δ 150.3 (d, $J = 15.8$, q), 141.4 (d, $J = 6.4$, q), 134.8 (d, $J = 6.5$, ArCH), 133.2 (d, $J = 7.3$, ArCH), 130.9 (d, $J = 2.0$, ArCH), 129.7 (s, ArCH), 129.5 (s, ArCH), 128.9 (s, ArCH), 128.8 (s, ArCH), 127.1 (d, $J = 5.4$, ArCH), 126.7 (dd, $J = 36.2$, 6.0, q), 64.4 (d, $J = 3.2$, $-\text{CH}_2-$), 64.3 (d, $J = 3.3$, $-\text{CH}_2-$), 38.1 (d, $J = 19.0$, q), 37.4 (t, $J = 4.3$, q), 31.3 (d, $J = 6.8$, $-\text{CH}_3$), 31.2 (d, $J = 6.8$, $-\text{CH}_3$). $^{31}\text{P}\{^1\text{H}\}$ NMR (CDCl_3 , 25 °C): δ 114.2 (d, $J = 466.2$, $-\text{P}(\text{O})-$), 66.4 (d, $J = 466.2$, $-\text{PR}_3$).

Preparation of $[\text{BuXPhosAu}]_2[\text{PO}_3\text{C}_5\text{H}_8\text{O}_3\text{P}]$ (13). General method B was followed using $(\text{BuXPhos})\text{AuCl}_4^t\text{Bu}$ (0.200 g, 0.265 mmol) and **1** (0.029 g, 0.13 mmol). The crude reaction mixture was dried under vacuum and extracted with benzene (30 mL). After filtering through diatomaceous earth, the solution was concentrated under vacuum until 5 mL remained. The addition of hexane (30 mL), followed by stirring for 30 min, resulted in the formation of a fine white solid, which was isolated through centrifugation and removal of the solution. The solid was dried under vacuum to afford 0.165 g (88%) of a white powder. HRMS ESI. Calcd for $\text{C}_{63}\text{H}_{99}\text{Au}_2\text{O}_6\text{P}_4$ [(M + H) $^+$]: m/z 1469.5719. Found: m/z 1469.5695. Anal. Calcd for $\text{C}_{63}\text{H}_{98}\text{Au}_2\text{O}_6\text{P}_4$: C, 51.50; H, 6.72. Found: C, 51.26; H, 6.32. ^1H NMR (CDCl_3 , 25 °C): δ 7.83 (brt, 2H, $J = 7.4$, ArH), 7.45 (m, 4H, ArH), 7.26 (m, 2H, ArH), 7.14 (brs, 4H, ArH), 4.10 (t, 2H, $J = 12.3$, $-\text{CH}_2-$), 4.03 (dd, 2H, $J = 14.5$, 11.5, $-\text{CH}_2-$), 3.73 (t, 2H, $J = 12.3$, $-\text{CH}_2-$), 3.66 (t, 2H, $J = 12.1$, $-\text{CH}_2-$), 2.99 (spt, 2H, $J = 6.9$, $^i\text{PrCH}$), 2.32 (m, 4H, $^i\text{PrCH}$), 1.40 (brd, 36H, $J = 14.9$, $-\text{CH}_3$), 1.32 (d, 6H, $J = 7.1$, $-\text{CH}_3$), 1.31 (d, 6H, $J = 7.0$, $-\text{CH}_3$), 1.29 (d, 12H, $J = 7.0$, $-\text{CH}_3$), 0.89 (d, 12H, $J = 6.7$, $-\text{CH}_3$). $^{13}\text{C}\{^1\text{H}\}$ NMR (CDCl_3 , 25 °C): δ 149.8 (s, quat), 148.5 (d, $J = 16.6$, quat), 145.7 (s, quat), 145.6 (s, quat), 135.7 (d, $J = 6.3$, ArCH), 135.1 (d, $J = 5.4$, quat), 134.9 (d, $J = 7.9$, ArCH), 130.4 (s, ArCH), 129.1 (dd, $J = 33.6$, 6.0, quat), 126.7 (d, $J = 5.6$, ArCH), 122.9 (s, ArCH), 122.5 (s, ArCH), 64.0 (d, $J = 3.7$, $-\text{CH}_2-$), 63.9 (d, $J = 4.0$, $-\text{CH}_2-$), 38.6 (d, $J = 19.8$, quat), 37.6 (brt, $J = 4.3$, quat), 33.5 (s, $^i\text{PrCH}$), 31.6 (d, $J = 6.5$, $-\text{CH}_3$), 31.23 (s, $^i\text{PrCH}$), 31.19 (s, $^i\text{PrCH}$), 26.63 (s, $-\text{CH}_3$), 26.61 (s, $-\text{CH}_3$), 23.9 (s, $-\text{CH}_3$), 23.6 (s, $-\text{CH}_3$), 23.41 (s, $-\text{CH}_3$), 23.37 (s, $-\text{CH}_3$). $^{31}\text{P}\{^1\text{H}\}$ NMR (CDCl_3 , 25 °C): δ 114.4 (d, $J = 473.5$, $-\text{P}(\text{O})-$), 64.6 (d, $J = 473.5$, $-\text{PR}_3$).

Preparation of Metallomacrocycles $[\text{Ph}_2\text{P}(\text{CH}_2)_2\text{O}(\text{CH}_2)_2\text{PPh}_2]\text{Au}_4[\text{PO}_3\text{C}_5\text{H}_8\text{O}_3\text{P}]_2$ (14). A vial (20 mL) was charged with **1** (0.0105 g, 0.0460 mmol), **11** (0.050 g, 0.045 mmol), and a magnetic stirring bar. After sealing with a septum and exchanging the atmosphere for nitrogen using a manifold, CH_3CN (18 mL) was added by syringe. The reaction mixture was heated (60 °C) in a block heater with stirring for 16 h. Without cooling, the reaction mixture was rapidly filtered through Celite into a scratched vial (20 mL). The vial was sealed with a septum, and the reaction mixture was concentrated under a nitrogen flow until it turned cloudy. After standing in a cabinet for 48 h, microcrystalline **14** was isolated by filtration and dried under vacuum (0.040 g, 83%). In some reactions, 1–3% of a secondary species was observed in the ^{31}P NMR spectrum even after multiple recrystallizations [CDCl_3 ; δ 112.3 (d), 35.3 (d), $^2J_{\text{PP}} = 528.1$ Hz] and was tentatively assigned as a trace of an alternate metallomacrocyclic. HRMS ESI. Calcd for $\text{C}_{66}\text{H}_{73}\text{Au}_4\text{O}_{14}\text{P}_8$ [(M + H) $^+$]: m/z 2125.1559. Found: m/z 2125.1477. Anal. Calcd for $\text{C}_{66}\text{H}_{72}\text{Au}_4\text{O}_{14}\text{P}_8$: C, 37.31; H, 3.42. Found: C, 36.98; H, 3.48. ^1H NMR (CDCl_3 , 25 °C): δ 7.72 (m, 16H, ArH), 7.51–7.38 (m, 24H, ArH), 4.15 (t, 4H, $J = 11.7$, $-\text{POCH}_2-$), 4.09 (t, 4H, $J = 12.6$, $-\text{POCH}_2-$), 3.99 (t, 4H, $J = 12.5$, $-\text{POCH}_2-$), 3.79 (t, 4H, $J = 12.7$, $-\text{POCH}_2-$), 3.73 (m, 4H, $-\text{OCH}_2-$), 3.60 (m, 4H, $-\text{OCH}_2-$), 3.04 (m, 4H, $-\text{CH}_2\text{P}-$), 2.68 (m, 4H, $-\text{CH}_2\text{P}-$). $^{13}\text{C}\{^1\text{H}\}$ NMR (CDCl_3 , 25 °C): δ 134.6 (d, $J = 13.5$, ArH), 133.1 (d, $J = 12.2$, ArH), 131.8 (s, ArH), 130.9 (s, ArH), 130.1 (d, $J = 50.7$, quat), 129.3 (d, $J = 48.8$, quat), 64.7 (br s, $-\text{OCH}_2-$), 64.5 (br s, $-\text{OCH}_2-$), 63.9 (br s, $-\text{OCH}_2-$), 37.1 (s, quat), 29.2 (d, $J = 30.3$, $-\text{CH}_2-$). $^{31}\text{P}\{^1\text{H}\}$ NMR (CDCl_3 , 25 °C): δ 111.2 (d, $J = 524.9$, $\text{P}-\text{O}-$), 35.6 (d, $J = 525.2$, PR_3).

NMR Monitoring Experiments. Bimetallic Complex and Metallomacrocyclic Synthesis. An NMR tube (5 mm) was charged with **1** (0.0050 g, 0.022 mmol) along with the mononuclear or dinuclear arylgold precursor (**2–11**; 2 equiv for **2** and **3**; 1 equiv for

4–11). After the atmosphere was exchanged for nitrogen using a manifold, DMSO-*d*₆ (0.5 mL) was injected by syringe.

Metallomacrocycle 14 with Estradiol. An NMR tube (5 mm) was charged with **14** (0.0055 g, 2.6 μmol) and estrogen (0.0007 g, 3 μmol) and capped with a rubber septum. After the atmosphere was exchanged for nitrogen using a manifold, CDCl₃ (freshly dried over CaH₂ and distilled) was injected by syringe.

X-ray Crystallography. Crystals were mounted on glass fibers. All measurements were made using graphite-monochromated Mo (9), Cu (10 and 13), or microfocus Cu (14) Kα radiation on a Bruker-AXS DUO three-circle diffractometer, equipped with an Apex II CCD detector. The initial space group determination was based on a matrix consisting of 36 or 120 frames. The data were reduced using SAINT⁷² and an empirical absorption correction was applied using SADABS.⁷³

Structures were solved using intrinsic phasing. Least-squares refinement for all structures was carried out on *F*². The non-hydrogen atoms were refined anisotropically. Hydrogen atoms were placed in riding positions and refined isotropically. Structure solution, refinement, and calculation of the derived results were performed using the SHELXTL package of computer programs⁷⁴ and ShelXle.⁷⁵ The X-ray structure of **14** required the use of PLATON SQUEEZE⁷⁶ to remove highly disordered solvent molecules, apparently consisting of the following: 3 molecules of DMSO, 1.5 molecules of dimethyl sulfide, and 1 molecule of water per unit cell. Details of the X-ray experiments are summarized in the Supporting Information.

■ ASSOCIATED CONTENT

Supporting Information

The Supporting Information is available free of charge on the ACS Publications website at DOI: 10.1021/acs.inorgchem.8b01805.

NMR and HRMS spectra and variable-temperature

NMR studies (PDF)

Accession Codes

CCDC 1839193 (13), 1839194 (10), 1839195 (9), and 1839196 (14) contain the supplementary crystallographic data for this paper. These data can be obtained free of charge via www.ccdc.cam.ac.uk/data_request/cif, or by emailing data_request@ccdc.cam.ac.uk, or by contacting The Cambridge Crystallographic Data Centre, 12 Union Road, Cambridge CB2 1EZ, UK; fax: +44 1223 336033.

■ AUTHOR INFORMATION

Corresponding Author

*E-mail: rstockla@bucknell.edu.

ORCID

Robert D. Pike: 0000-0002-8712-0288

Robert A. Stockland, Jr.: 0000-0002-4351-6395

Notes

The authors declare no competing financial interest.

■ ACKNOWLEDGMENTS

The authors acknowledge the National Science Foundation for generous support of this work (Grant CHE-1300088) as well as the funds to purchase the NMR spectrometer (Grant CHE-0521108) and are indebted to the NSF (Grant CHE-0443345) and the College of William and Mary for the purchase of the X-ray equipment. The authors thank Brian Smith and Hasan Arslan for helpful discussions.

■ REFERENCES

- (1) Gagnon, K. J.; Perry, H. P.; Clearfield, A. Conventional and Unconventional Metal-Organic Frameworks Based on Phosphonate Ligands: MOFs and UMOFs. *Chem. Rev.* **2012**, *112*, 1034–1054.
- (2) Alberti, G.; Casciola, M.; Costantino, U.; Vivani, R. Layered and Pillared Metal(IV) Phosphates and Phosphonates. *Adv. Mater.* **1996**, *8*, 291–303.
- (3) Goura, J.; Chandrasekhar, V. Molecular Metal Phosphonates. *Chem. Rev.* **2015**, *115*, 6854–6965.
- (4) Ma, T.-Y.; Yuan, Z.-Y. Metal Phosphonate Hybrid Mesostructures: Environmentally Friendly Multifunctional Materials for Clean Energy and Other Applications. *ChemSusChem* **2011**, *4*, 1407–1419.
- (5) Murugavel, R.; Choudhury, A.; Walawalkar, M. G.; Pothiraja, R.; Rao, C. N. R. Metal Complexes of Organophosphate Esters and Open-Framework Metal Phosphates: Synthesis, Structure, Transformations, and Applications. *Chem. Rev.* **2008**, *108*, 3549–3655.
- (6) Roundhill, D. M.; Sperline, R. F.; Beaulieu, W. B. Metal Complexes of Substituted Phosphinites and Secondary Phosphites. *Coord. Chem. Rev.* **1978**, *26*, 263–279.
- (7) Zipp, A. P. The Behavior of the Tetra-μ-Pyrophosphito-Diplatinum(II) Ion Pt₂(P₂O₅H₂)^{−4} and Related Species. *Coord. Chem. Rev.* **1988**, *84*, 47–83.
- (8) Kläui, W.; Neukomm, H.; Werner, H.; Huttner, G. [π-C₅H₅Co{P(OR)₂O}₃BF₄]₃BF₄ - Synthesis, Structure, and Reactivity of (Cyclopentadienyl)Cobalt Complexes Containing New Cage-Forming Phosphite Chelating Ligands. *Chem. Ber.* **1977**, *110*, 2283–2289.
- (9) Kläui, W. The Coordination Chemistry and Organometallic Chemistry of Tridentate Oxygen Ligands with π-Donor Properties. *Angew. Chem., Int. Ed. Engl.* **1990**, *29*, 627–637.
- (10) Kläui, W.; Asbahr, H.-O.; Schramm, G.; Englert, U. Tris-Chelating Oxygen Ligands: New Synthetic Routes to Sterically Demanding Ligands. *Chem. Ber.* **1997**, *130*, 1223–1229.
- (11) Hanson, S. K.; Mueller, A. H.; Oldham, W. J., Jr. Kläui Ligand Thin Films for Rapid Plutonium Analysis by Alpha Spectrometry. *Anal. Chem.* **2014**, *86*, 1153–1159.
- (12) Allen, K. J. H.; Nicholls-Allison, E. C.; Johnson, K. R. D.; Nirwan, R. S.; Berg, D. J.; Wester, D.; Twamley, B. Lanthanide Complexes of the Kläui Metalloligand, CpCo(P=O(OR)₂)₃: An Examination of Ligand Exchange Kinetics between Isotopomers by Electrospray Mass Spectrometry. *Inorg. Chem.* **2012**, *51*, 12436–12443.
- (13) Baudry, D.; Ephritikhine, M.; Kläui, W.; Lance, M.; Nierlich, M.; Vigner, J. Uranium(IV) Complexes with the Oxygen Tripod Ligand L[−] = CpCo[P(O)(OEt)₂]₃[−]. X-Ray Crystal-Structure of L₂UCl₂. *Inorg. Chem.* **1991**, *30*, 2333–2336.
- (14) Krishnan, V. M.; Arman, H. D.; Tonzetich, Z. J. Synthesis and Characterisation of Ruthenium-Nitrosyl Complexes in Oxygen-Rich Ligand Environments. *Dalton Trans.* **2017**, *46*, 1186–1193.
- (15) Leung, W.-H.; Zhang, Q.-F.; Yi, X.-Y. Recent Developments in the Coordination and Organometallic Chemistry of Kläui Oxygen Tripodal Ligands. *Coord. Chem. Rev.* **2007**, *251*, 2266–2279.
- (16) Wang, G.; Yi, X.; Williams, I. D.; Leung, W. Synthesis and Structure of a Bismuth(III)/Chromium(VI) Oxo Cluster Containing a Bi₄Cr₄O₁₂ Core. *Inorg. Chem.* **2011**, *50*, 9141–9146.
- (17) Schneemann, A.; Bon, V.; Schwedler, I.; Senkovska, I.; Kaskel, S.; Fischer, R. A. Flexible Metal-Organic Frameworks. *Chem. Soc. Rev.* **2014**, *43*, 6062–6096.
- (18) Lin, Z.-J.; Lu, J.; Hong, M.; Cao, R. Metal-Organic Frameworks Based on Flexible Ligands (FL-MOFs): Structures and Applications. *Chem. Soc. Rev.* **2014**, *43*, 5867–5895.
- (19) Zheng, Y.-Q.; Lin, J.-L.; Kong, Z.-P. Coordination Polymers Based on Cobridging of Rigid and Flexible Spacer Ligands: Syntheses, Crystal Structures, and Magnetic Properties of Mn(bpy)(H₂O)-(C₄H₄O₄)]·0.5bpy, Mn(bpy)(C₅H₄O₄), and Mn(bpy)(C₆H₈O₄). *Inorg. Chem.* **2004**, *43*, 2590–2596.
- (20) Amghouz, Z.; Rocas, L.; Garcia-Granda, S.; Garcia, J. R.; Souhail, B.; Mafra, L.; Shi, F.; Rocha, J. Metal Organic Frameworks

Assembled from Y(III), Na(I), and Chiral Flexible-Achiral Rigid Dicarboxylates. *Inorg. Chem.* **2010**, *49*, 7917–7926.

(21) Lord, T. M.; Casino, S. L.; Hartzell, S. E.; Garcia, K. J.; Pike, R. D.; Stockland, R. A., Jr. Convenient Access to Arylated Spirocyclic Bisphosphonates. *ChemistrySelect* **2016**, *1*, 2188–2191.

(22) Pike, R. D.; Reinecke, B. A.; Dellinger, M. E.; Wiles, A. B.; Harper, J. D.; Cole, J. R.; Dendramis, K. A.; Borne, B. D.; Harris, J. L.; Pennington, W. T. Bicyclic Phosphite Esters from Pentaerythritol and Dipentaerythritol: New Bridging Ligands in Organometallic and Inorganic Chemistry. *Organometallics* **2004**, *23*, 1986–1990.

(23) Cook, T. R.; Stang, P. J. Recent Developments in the Preparation and Chemistry of Metallacycles and Metallocages via Coordination. *Chem. Rev.* **2015**, *115*, 7001–7045.

(24) Chakrabarty, R.; Mukherjee, P. S.; Stang, P. J. Supramolecular Coordination: Self-Assembly of Finite Two- and Three-Dimensional Ensembles. *Chem. Rev.* **2011**, *111*, 6810–6918.

(25) McConnell, A. J.; Wood, C. S.; Neelakandan, P. P.; Nitschke, J. R. Stimuli-Responsive Metal-Ligand Assemblies. *Chem. Rev.* **2015**, *115*, 7729–7793.

(26) Wang, W.; Wang, Y.-X.; Yang, H.-B. Supramolecular Transformations within Discrete Coordination-Driven Supramolecular Architectures. *Chem. Soc. Rev.* **2016**, *45*, 2656–2693.

(27) Troev, K. D. Reactivity of P–H Group of Phosphorus Based Compounds. *Acidity and Tautomerization of P–H Group*; Academic Press, 2018; pp 1–17.

(28) Janesko, B. G.; Fisher, H. C.; Bridle, M. J.; Montchamp, J.-L. P(=O)H to P-OH Tautomerism: A Theoretical and Experimental Study. *J. Org. Chem.* **2015**, *80*, 10025–10032.

(29) Roth, K. E.; Blum, S. A. Relative Kinetic Basicities of Organogold Compounds. *Organometallics* **2010**, *29*, 1712–1716.

(30) BabaAhmadi, R.; Ghanbari, P.; Rajabi, N. A.; Hashmi, A. S. K.; Yates, B. F.; Ariafard, A. A Theoretical Study on the Protodeauration Step of the Gold(I)-Catalyzed Organic Reactions. *Organometallics* **2015**, *34*, 3186–3195.

(31) Gaggioli, C. A.; Ciancaleoni, G.; Zuccaccia, D.; Bistoni, G.; Belpassi, L.; Tarantelli, F.; Belanzoni, P. Strong Electron-Donating Ligands Accelerate the Protodeauration Step in Gold(I)-Catalyzed Reactions: A Quantitative Understanding of the Ligand Effect. *Organometallics* **2016**, *35*, 2275–2285.

(32) Wang, W.; Hammond, G. B.; Xu, B. Ligand Effects and Ligand Design in Homogeneous Gold(I) Catalysis. *J. Am. Chem. Soc.* **2012**, *134*, 5697–5705.

(33) Wang, W.; Kumar, M.; Hammond, G. B.; Xu, B. Enhanced Reactivity in Homogeneous Gold Catalysis through Hydrogen Bonding. *Org. Lett.* **2014**, *16*, 636–639.

(34) Manbeck, G. F.; Kohler, M. C.; Porter, M. R.; Stockland, R. A., Jr. P-H Activation using Alkynylgold Substrates: Steric and Electronic Effects. *Dalton Trans.* **2011**, *40*, 12595–12606.

(35) Richard, M. E.; Ciccarelli, R. M.; Garcia, K. J.; Miller, E. J.; Casino, S. L.; Pike, R. D.; Stockland, R. A., Jr. Stereospecific Protodeauration/Transmetalation Generating Configurationally Stable P-Metalated Nucleoside Derivatives. *Eur. J. Org. Chem.* **2018**, *2018*, 2167–2170.

(36) Hollatz, C.; Schier, A.; Schmidbaur, H. Gold(I) Complexes with P=O and P-OH Functionalised Phosphorus Ligands. *Inorg. Chim. Acta* **2000**, *300–302*, 191–199.

(37) Hollatz, C.; Schier, A.; Schmidbaur, H. Neutral Gold(I) Complexes with Mixed Phosphorus Ligands. *Chem. Ber.* **1997**, *130*, 1333–1338.

(38) Partyka, D. V. Transmetalation of Unsaturated Carbon Nucleophiles from Boron-Containing Species to the Mid to Late d-Block Metals of Relevance to Catalytic C–X Coupling Reactions (X = C, F, N, O, Pb, S, Se, Te). *Chem. Rev.* **2011**, *111*, 1529–1595.

(39) Partyka, D. V.; Zeller, M.; Hunter, A. D.; Gray, T. G. Arylgold(I) Complexes from Base-Assisted Transmetalation: Structures, NMR Properties, and Density-Functional Theory Calculations. *Inorg. Chem.* **2012**, *51*, 8394–8401.

(40) Gao, L.; Peay, M. A.; Partyka, D. V.; Updegraff, J. B., III; Teets, T. S.; Esswein, A. J.; Zeller, M.; Hunter, A. D.; Gray, T. G. Mono- and

Di-Gold(I) Naphthalenes and Pyrenes: Syntheses, Crystal Structures, and Photophysics. *Organometallics* **2009**, *28*, 5669–5681.

(41) Puddephatt, R. J. Macrocycles, Catenanes, Oligomers and Polymers in Gold Chemistry. *Chem. Soc. Rev.* **2008**, *37*, 2012–2027.

(42) Schmidbaur, H.; Schier, A. Auophilic Interactions as a Subject of Current Research: An Up-Date. *Chem. Soc. Rev.* **2012**, *41*, 370–412.

(43) Sutra, P.; Igau, A. Anionic Phosph(in)ito ("Phosphoryl") Ligands: Non-Classical "Actor" Phosphane-Type Ligands in Coordination Chemistry. *Coord. Chem. Rev.* **2016**, *308*, 97–116.

(44) Lebon, E.; Sylvain, R.; Piau, R. E.; Lanthony, C.; Pilme, J.; Sutra, P.; Boggio-Pasqua, M.; Heully, J.-L.; Alary, F.; Juris, A.; Igau, A. Phosphoryl Group as a Strong σ -Donor Anionic Phosphine-Type Ligand: A Combined Experimental and Theoretical Study on Long-Lived Room Temperature Luminescence of the Ru(tpy)(bpy)-(Ph₂PO)]⁺ Complex. *Inorg. Chem.* **2014**, *53*, 1946–1948.

(45) Leyva-Perez, A.; Cabrero-Antonino, J. R.; Cantin, A.; Corma, A. Gold(I) Catalyzes the Intermolecular Hydroamination of Alkynes with Imines and Produces α,α' -N-Triarylbenzenamines: Studies on their use as Intermediates in Synthesis. *J. Org. Chem.* **2010**, *75*, 7769–7780.

(46) Strasser, C. E.; Cronje, S.; Schmidbaur, H.; Raubenheimer, H. G. The Preparation, Properties and X-Ray Structures of Gold(I) Trithiophosphite Complexes. *J. Organomet. Chem.* **2006**, *691*, 4788–4796.

(47) Green, M. L. H. A New Approach to the Formal Classification of Covalent Compounds of the Elements. *J. Organomet. Chem.* **1995**, *500*, 127–148.

(48) Brandys, M.-C.; Puddephatt, R. J. Polymers and Rings in Gold(I) Diphosphine Complexes: Linking Gold Rings through Auophilic Interactions. *Chem. Commun.* **2001**, 1280–1281.

(49) A yield was not determined for this example because of the intractable nature of the crude reaction mixture.

(50) Lim, S. H.; Schmitt, J. C.; Shearer, J.; Jia, J.; Olmstead, M. M.; Fetting, J. C.; Balch, A. L. Crystallographic and Computational Studies of Luminescent, Binuclear Gold(I) Complexes, Au₂(Ph₂P(CH₂)_nPPh₂)₂I₂ (n = 3–6). *Inorg. Chem.* **2013**, *52*, 823–831.

(51) Wang, Q.; Cheng, M.; Xiong, S.; Hu, X.-Y.; Jiang, J.; Wang, L.; Pan, Y. P=O Functional Group-Containing Cryptands: From Supramolecular Complexes to Poly[2]Pseudorotaxanes. *Chem. Commun.* **2015**, *51*, 2667–2670.

(52) Liu, L.; Liu, Y.; Liu, P.; Wu, J.; Guan, Y.; Hu, X.; Lin, C.; Yang, Y.; Sun, X.; Ma, J.; Wang, L. Phosphine Oxide Functional Group Based Three-Station Molecular Shuttle. *Chem. Sci.* **2013**, *4*, 1701–1706.

(53) Erbas-Cakmak, S.; Leigh, D. A.; McTernan, C. T.; Nussbaumer, A. L. Artificial Molecular Machines. *Chem. Rev.* **2015**, *115*, 10081–10206.

(54) Ahmed, R.; Altieri, A.; D'Souza, D. M.; Leigh, D. A.; Mullen, K. M.; Papmeyer, M.; Slawin, A. M. Z.; Wong, J. K. Y.; Woollins, J. D. Phosphorus-Based Functional Groups as Hydrogen Bonding Templates for Rotaxane Formation. *J. Am. Chem. Soc.* **2011**, *133*, 12304–12310.

(55) Zhou, J.; Yu, G.; Huang, F. Supramolecular Chemotherapy Based on Host-Guest Molecular Recognition: A Novel Strategy in the Battle Against Cancer with a Bright Future. *Chem. Soc. Rev.* **2017**, *46*, 7021–7053.

(56) Wang, Q.; Zhang, P.; Xu, J.; Xia, B.; Tian, L.; Chen, J.; Li, J.; Lu, F.; Shen, Q.; Lu, X.; Huang, W.; Fan, Q. NIR-Absorbing Dye Functionalized Supramolecular Vesicles for Chemo-Photothermal Synergistic Therapy. *ACS Appl. Bio Mater.* **2018**, *1*, 70–78.

(57) Shangguan, L.; Chen, Q.; Shi, B.; Huang, F. Enhancing the Solubility and Bioactivity of Anticancer Drug Tamoxifen by Water-Soluble Pillar[6]Arene-Based Host-Guest Complexation. *Chem. Commun.* **2017**, *53*, 9749–9752.

(58) Modro, A. M.; Modro, T. A. The Phosphoryl and the Carbonyl Group as Hydrogen Bond Acceptors. *Can. J. Chem.* **1999**, *77*, 890–894.

- (59) Tupikina, E. Y.; Bodensteiner, M.; Tolstoy, P. M.; Denisov, G. S.; Shenderovich, I. G. P=O Moiety as an Ambidextrous Hydrogen Bond Acceptor. *J. Phys. Chem. C* **2018**, *122*, 1711–1720.
- (60) Li, Q.-S.; Wan, C.-Q.; Zou, R.-Y.; Xu, F.-B.; Song, H.-B.; Wan, X.-J.; Zhang, Z.-Z. Gold(I) η^2 -Arene Complexes. *Inorg. Chem.* **2006**, *45*, 1888–1890.
- (61) Partyka, D. V.; Robilotto, T. J.; Zeller, M.; Hunter, A. D.; Gray, T. G. Dialkylbiarylphosphine Complexes of Gold(I) Halides. Gold–Aryl π -Interactions in the Solid State. *Organometallics* **2008**, *27*, 28–32.
- (62) Schmidbaur, H.; Schier, A. Gold η^2 -Coordination to Unsaturated and Aromatic Hydrocarbons: The Key Step in Gold-Catalyzed Organic Transformations. *Organometallics* **2010**, *29*, 2–23.
- (63) Ni, Q.-L.; Jiang, X.-F.; Huang, T.-H.; Wang, X.-J.; Gui, L.-C.; Yang, K.-G. Gold(I) Chloride Complexes of Polyphosphine Ligands with Electron-Rich Arene Spacer: Gold–Arene Interactions. *Organometallics* **2012**, *31*, 2343–2348.
- (64) Muller, N.; Reiter, R. C. Temperature Dependence of Chemical Shifts of Protons in Hydrogen Bonds. *J. Chem. Phys.* **1965**, *42*, 3265–3269.
- (65) Bardají, M.; de la Cruz, M. T.; Jones, P. G.; Laguna, A.; Martínez, J.; Villacampa, M. D. Luminescent Dinuclear Gold Complexes of Bis(Diphenylphosphano)Acetylene. *Inorg. Chim. Acta* **2005**, *358*, 1365–1372.
- (66) Ramírez, J.; Sanaú, M.; Fernández, E. Gold(0) Nanoparticles for Selective Catalytic Diboration. *Angew. Chem., Int. Ed.* **2008**, *47*, 5194–5197.
- (67) Brandys, M.-C.; Jennings, M. C.; Puddephatt, R. J. Luminescent Gold(I) Macrocycles with Diphosphine and 4,4'-Bipyridyl Ligands. *J. Chem. Soc., Dalton Trans.* **2000**, 4601–4606.
- (68) Pintado-Alba, A.; de la Riva, H.; Nieuwhuyzen, M.; Bautista, D.; Raithby, P. R.; Sparkes, H. A.; Teat, S. J.; Lopez-de-Luzuriaga, J. M.; Lagunas, M. C. Effects of Diphosphine Structure on Auophilicity and Luminescence in Au(I) Complexes. *Dalton Trans.* **2004**, 3459–3467.
- (69) Foley, J. B.; Bruce, A. E.; Bruce, M. R. M. An Unprecedented Photochemical Cis to Trans Isomerization of Dinuclear Gold(I) Bis(Diphenylphosphino) Ethylene Complexes. *J. Am. Chem. Soc.* **1995**, *117*, 9596–9597.
- (70) Zhang, Q.-F.; Williard, P. G.; Wang, L.-S. Polymorphism of Phosphine-Protected Gold Nanoclusters: Synthesis and Characterization of a New 22-Gold-Atom Cluster. *Small* **2016**, *12*, 2518–2525.
- (71) Lenker, H. K.; Gray, T. G.; Stockland, R. A., Jr. Rapid Synthesis of Arylgold Compounds using Dielectric Heating. *Dalton Trans.* **2012**, *41*, 13274–13276.
- (72) SAINT+; Bruker Analytical X-ray Systems: Madison, WI, 2001.
- (73) SADABS; Bruker Analytical X-ray Systems: Madison, WI, 2001.
- (74) Sheldrick, G. M. A Short History of SHELX. *Acta Crystallogr., Sect. A: Found. Crystallogr.* **2008**, *64*, 112–122.
- (75) Huebschle, C. B.; Sheldrick, G. M.; Dittrich, B. ShelXle: A Qt Graphical User Interface for SHELXL. *J. Appl. Crystallogr.* **2011**, *44*, 1281–1284.
- (76) Spek, A. L. PLATON SQUEEZE: A Tool for the Calculation of the Disordered Solvent Contribution to the Calculated Structure Factors. *Acta Crystallogr., Sect. C: Struct. Chem.* **2015**, *71*, 9–18.